Design of Simulated-Moving-Bed Chromatography with Enriched Extract Operation (EE-SMB): Langmuir Isotherms

ARTICLE *in* INDUSTRIAL & ENGINEERING CHEMISTRY RESEARCH · AUGUST 2006

Impact Factor: 2.59 · DOI: 10.1021/ie060256z

3 AUTHORS, INCLUDING:

Hyun-Ku Rhee
Seoul National University
171 PUBLICATIONS **2,541** CITATIONS

Design of Simulated Moving Bed Separations: Generalized Langmuir Isotherm

Marco Mazzotti*

Institute of Process Engineering, ETH Zurich, Sonneggstrasse 3, CH-8092 Zurich, Switzerland

In this paper, exact criteria for the complete separation of binary mixtures in simulated moving bed (SMB) units are developed. They apply to systems subject to the generalized Langmuir isotherm, whose definition yields four different types of isotherms corresponding to different combinations of Langmuir and anti-Langmuir behavior of the components to be separated. These criteria are derived in a similar way in the different cases using the equilibrium theory of chromatography applied to the equivalent true moving bed (TMB) unit. Separation performance is controlled by the dimensionless flow rate ratios. The complete separation region in the operating parameters space has boundaries that are constituted of straight lines and curves, defined through simple and easy-to-use equations. These in turn depend on the adsorption isotherm parameters and on the composition of the feed mixture. The analogies and differences observed among the four isotherms in terms of complete separation region are analyzed and discussed.

1. Introduction

The simulated moving bed (SMB) technique, whose scheme is shown in Figure 1, is an adsorption-based separation process that entails the operation of a set of adsorption beds, or chromatographic columns, to allow for the continuous separation of a feed mixture, typically in two fractions. This technology is applied at widely different scales for the separation of hydrocarbons and sugars as well as of fine chemicals, particularly enantiomers, and of biopharmaceuticals.[1−3] The model-based design and development of new SMB applications is an established approach, and models of different levels of complexity are used, either detailed models for simulation and optimization or simplified models for short-cut design purposes. More recently, even model predictive control has been developed and successfully applied to SMBs.[4,5]

In the context of the use of simplified models, the application of the equilibrium theory of chromatography[6] to the design of SMB separations has led to particularly powerful results.[7,8] The equilibrium theory has allowed the identification of the key dimensionless parameters, i.e., the flow rate ratios, controlling separation performance, and the partitioning of the operating parameter space into regions attaining different separation regimes. Of special importance is of course the complete separation region, which in the case of the Langmuir isotherm is defined by a set of user-friendly algebraic relationships and is often graphically presented in the two-dimensional plane having the flow rate ratios in the two central sections of the SMB unit as coordinates. Such results have elucidated a number of important effects in SMB separations and are a standard design tool in academia and industry. Important extensions have been made by determining criteria for the design of the separation of mixtures subject to the bi-Langmuir isotherm[9,10] and to the multicomponent competitive Langmuir isotherm,[11,12] as well as for the design of gradient SMB separations[13−15] and of three fraction separations.[16]

The equilibrium theory based approach has been developed so far only for systems subject to Langmuir-like isotherms, namely favorable competitive isotherms. In other cases, which are important for applications, extensive numerical simulations have been carried out to determine the region of complete separation.[17] This is of course a fully legitimate approach that brings however lesser insight than the one based on exact solutions of the equilibrium theory model of SMBs. It is certainly desirable to extend the equilibrium theory approach to the largest possible number of cases, covering also situations where the retention behavior of the species to be separated deviates in a significant way from the Langmuir behavior.

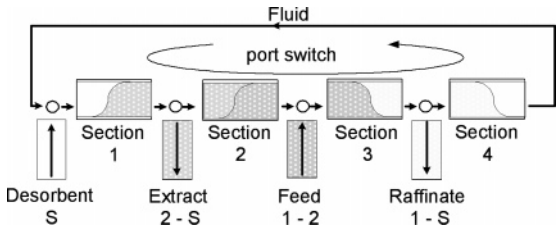

Figure 1. Scheme of a four-section simulated moving bed unit for the separation of a binary mixture of components 1 (less retained) and 2 (more retained) in an inert solvent (S).

This is now possible by exploiting the results recently obtained through the application of the equilibrium theory to a generalized Langmuir isotherm. Such an isotherm allows the combination of species that are either Langmuir-like or anti-Langmuir-like, i.e., four combinations in the case of binary systems, thus leading to quite different chromatographic behaviors. In this paper, we present the application of the equilibrium theory to the SMB separation of binary systems subject to the generalized Langmuir isotherm, and we show how all the results that had been earlier obtained for the Langmuir isotherm extend to the generalized Langmuir isotherm. In particular, it is possible to identify a complete separation region in the operating parameter space, whose boundaries are defined by a set of simple algebraic relationships as a function of the adsorption isotherm parameters and of the composition of the feed.

The paper is organized as follows. First, the key results about the application of the equilibrium theory to the generalized Langmuir isotherm are summarized. Then, the conditions to achieve complete separation in a SMB process are obtained, first in implicit form and then in a form that allows for an exact definition of the boundaries of the complete separation region in the operating parameter space. All the results obtained in this work are thoroughly demonstrated, but for the sake of readability, some of the proofs are confined to the appendices at the end of the article.

* To whom correspondence should be addressed. E-mail: marco.mazzotti@ipe.mavt.ethz.ch. Tel.: +41-44-6322456. Fax: +41-44-6321141.

10.1021/ie060298n CCC: $33.50
Published on Web 08/03/2006

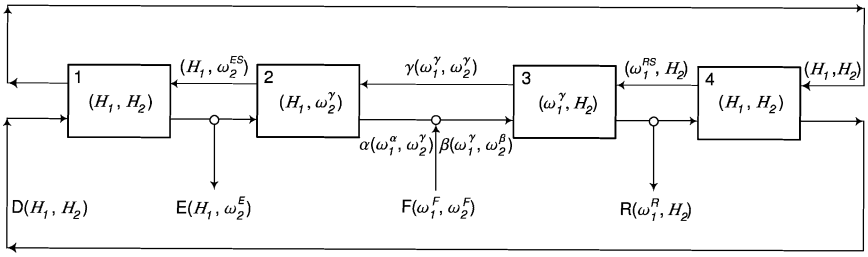

Figure 2. Four-section true moving bed unit with indication of the composition states compatible with complete separation. The composition states are characterized by the corresponding ω vectors, which are formally the same for all four generalized Langmuir isotherms.

2. Background

2.1. Design Problem. Let us consider a four-section simulated moving bed (SMB) unit and its equivalent true moving bed (TMB) unit, where a binary mixture is to be separated in an isocratic mode in such a way to have only component 1, i.e., the less adsorbable one, in the raffinate and only component 2, i.e., the more adsorbable one, in the extract. We intend to design SMB operating conditions for complete separation and, to this aim, to exploit the equivalence between TMB and SMB, which is guaranteed by the following relationships:

$$Q_j^{\mathrm{SMB}} = Q_j^{\mathrm{TMB}} + Q_{\mathrm{S}}\frac{\epsilon_{\mathrm{b}}}{1-\epsilon_{\mathrm{b}}} \quad (j = 1, ..., 4) \tag{1}$$

$$Q_{\mathrm{S}} = (1-\epsilon_{\mathrm{b}})\frac{V}{t^*} \tag{2}$$

where Q_j is the volumetric flow rate in section j; Q_{S} is the solid flow rate in the TMB unit; V and ϵ_{b} are column volume and void fraction; and t^* is the switch time for the SMB unit. On the basis of these, the cyclic steady state of an SMB unit can be studied by considering the steady state of the equivalent TMB unit, which is shown in Figure 2.

In the frame of equilibrium theory, the separation performance of a TMB, hence of an SMB, is controlled by the dimensionless flow rate ratios, which can be defined as follows in terms of SMB or TMB operating parameters:

$$m_j = \frac{Q_j^{\mathrm{SMB}}t^* - \epsilon^* V}{V(1-\epsilon^*)} = \frac{Q_j^{\mathrm{TMB}} - \epsilon_{\mathrm{p}}Q_{\mathrm{S}}}{Q_{\mathrm{S}}(1-\epsilon_{\mathrm{p}})} \quad (j = 1, ..., 4) \tag{3}$$

where the overall column void fraction ϵ^* is defined in terms of column void fraction, ϵ_{b}, and particle porosity, ϵ_{p}, as $\epsilon^* = \epsilon_{\mathrm{b}} + (1-\epsilon_{\mathrm{b}})\epsilon_{\mathrm{p}}$. This property of the m_j parameters is due to the fact that within each countercurrent section the flow rate ratio controls the state that is attained at steady state, as discussed in section 2.3.

Within each countercurrent section j of the TMB unit, the net flow rate of species i, F_i^j, is defined as

$$F_i^j = Q_{\mathrm{S}}(1-\epsilon_{\mathrm{p}})(m_j c_i^j - n_i^j) = Q_{\mathrm{S}}(1-\epsilon_{\mathrm{p}})f_i^j \quad (i = 1, 2; j = 1, ..., 4) \tag{4}$$

where the concentrations are those attained within the section at steady state and f_i^j is a quantity that is proportional to and has the same sign as F_i^j.

2.2. Generalized Langmuir Isotherm. Let us consider binary systems where adsorption is characterized by the generalized Langmuir isotherm introduced recently,[18] i.e., by the following adsorption isotherm:

$$n_i = N_i K_i c_i/\delta \quad (i = 1, 2) \tag{5}$$

where c_i and n_i are fluid and adsorbed phase concentrations, respectively, and the denominator is defined as

$$\delta = 1 + p_1 K_1 c_1 + p_2 K_2 c_2 \tag{6}$$

In the equations above, K_i and N_i are the equilibrium constant and the saturation loading capacity of the ith component, respectively; $H_i = N_i K_i$ is its Henry's constant, i.e., the infinite dilution slope of its isotherm; p_1 and p_2 can take the values ± 1, and through these, the sign of the corresponding term in the denominator can be assigned. Langmuirian, favorable behavior corresponds to $p_i = 1$, whereas anti-Langmuirian, unfavorable behavior requires $p_i = -1$. Equations 5 and 6 define four different isotherms for the same values K_i and N_i: the standard Langmuir isotherm, labeled **L**, where $p_1 = p_2 = 1$; the anti-Langmuir isotherm, **A**, where $p_1 = p_2 = -1$; the mixed Langmuir isotherm, $\mathbf{M}_1$, where $p_1 = 1$ and $p_2 = -1$; and the mixed Langmuir isotherm, $\mathbf{M}_2$, where $p_1 = -1$ and $p_2 = 1$. In all cases, we will consider feed compositions that fulfill the requirement $\delta > 0$. Moreover, in the case of the mixed Langmuir isotherm $\mathbf{M}_2$, feed compositions must fulfill the following additional constraints:

$$\begin{gathered} c_1^F < k \\ c_2^F < k/h \\ 0 < (c_1^F - k + hc_2^F)^2 - 4hc_1^F c_2^F \end{gathered} \tag{7}$$

where $h = N_1/N_2$ and $k = (1 - H_1/H_2)/K_1$.

The quadratic equation

$$F(\omega) = \frac{p_1 K_1 n_1}{H_1 - \omega} + \frac{p_2 K_2 n_2}{H_2 - \omega} = 1 \tag{8}$$

where n_1 and n_2 are given by the adsorption isotherm (eq 5), defines a one-to-one mapping between (c_1, c_2) and (ω_1,ω_2). If either $c_1 = 0$ or $c_2 = 0$, the equation above reduces to a first-order equation and yields only one ω value, whereas the other ω value equals either H_1 or H_2, respectively. It has been shown that ω_1 and ω_2 are always positive and that their values belong to the following intervals:[18]

$$\text{case } \mathbf{L}: \quad 0 < \omega_1 \le H_1 \le \omega_2 \le H_2 \tag{9}$$

$$\text{case } \mathbf{A}: \quad H_1 \le \omega_1 \le H_2 \le \omega_2 < +\infty \tag{10}$$

$$\text{case } \mathbf{M_1}: \quad 0 < \omega_1 \le H_1 < H_2 \le \omega_2 < +\infty \tag{11}$$

$$\text{case } \mathbf{M_2}: \quad H_1 \le \omega_1 \le \omega_2 \le H_2 \tag{12}$$

It is worth noting that for the mixed case $\mathbf{M}_2$ only the region where the feed states belong, as specified earlier through eqs 7, has been considered in eq 12. A more general treatment of the mixed Langmuir isotherm $\mathbf{M}_2$ has been presented elsewhere,

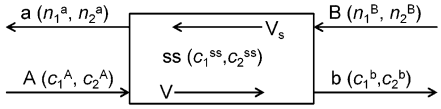

Figure 3. Scheme of a moving bed countercurrent adsorber.

where the region of the composition space considered here is called region 1.[18,19]

The following equations provide the inverse relationships of the one-to-one mapping, thus giving c_1 and c_2 in terms of ω_1 and ω_2:

$$K_1 c_1 = \frac{-p_1 H_2(\omega_1 - H_1)(\omega_2 - H_1)}{\omega_1\omega_2(H_2 - H_1)} \tag{13}$$

$$K_2 c_2 = \frac{p_2 H_1(\omega_1 - H_2)(\omega_2 - H_2)}{\omega_1\omega_2(H_2 - H_1)} \tag{14}$$

From these, corresponding expressions for δ, n_1, and n_2 can be easily derived:

$$\delta = \frac{H_1 H_2}{\omega_1\omega_2} \tag{15}$$

$$K_1 n_1 = \frac{-p_1(\omega_1 - H_1)(\omega_2 - H_1)}{H_2 - H_1} \tag{16}$$

$$K_2 n_2 = \frac{p_2(\omega_1 - H_2)(\omega_2 - H_2)}{H_2 - H_1} \tag{17}$$

2.3. Moving Bed Chromatographic Column. Let us consider the single moving bed chromatographic column of Figure 3, which is the building block of a TMB unit, and the following piecewise constant initial value problem (Riemann problem):

$$\text{at} \quad \tau = 0,\ 0 \le x \le 1: \quad c_i = c_i^0 \ (\omega_i = \omega_i^0), \quad \text{(state 0)} \tag{18}$$

$$\text{at} \quad x = 0,\ \tau > 0: \quad c_i = c_i^A \ (\omega_i = \omega_i^A), \quad \text{(state } A\text{)} \tag{19}$$

$$\text{at} \quad x = 1,\ \tau > 0: \quad n_i = n_i^B \ (\omega_i = \omega_i^B), \ \text{(state } B\text{)} \tag{20}$$

where τ and x are dimensionless time and space coordinates; the first condition is the initial state in the column, the second one is the state of the incoming fluid at the left end of the column, and the third is the state of the incoming solid phase at the right end of the column. The ω_i values are calculated in terms of the composition through eqs 5 and 8.

For the design of TMB units, only the steady-state (infinite time) solution of the Riemann problem is of interest. This is controlled by the flow rate ratio m, according to the following scheme, which is the same for all four generalized Langmuir isotherms:[18]

$$\text{state } B, (\omega_1^B,\omega_2^B) \quad \text{if} \quad m\delta_B \le \min\{\omega_1^A,\omega_1^B\} \tag{21}$$

$$\text{state } T_1, (\omega_1^{T_1},\omega_2^B) \quad \text{if} \quad \omega_1^B < \omega_1^{T_1} < \omega_1^A \text{ and } m\delta_{T_1} = \omega_1^{T_1} \tag{22}$$

$$\text{state } I, (\omega_1^A,\omega_2^B) \quad \text{if} \quad \max\{\omega_1^A,\omega_1^B\} \le m\delta_I \le \min\{\omega_2^A,\omega_2^B\} \tag{23}$$

$$\text{state } T_2, (\omega_1^A,\omega_2^{T_2}) \quad \text{if} \quad \omega_2^B < \omega_2^{T_2} < \omega_2^A \text{ and } m\delta_{T_2} = \omega_2^{T_2} \tag{24}$$

$$\text{state } A, (\omega_1^A,\omega_2^A) \quad \text{if} \quad \max\{\omega_2^A,\omega_2^B\} \le m\delta_A \tag{25}$$

There are always three possible steady states, i.e., the inlet fluid and solid states, A and B, and the intermediate state I, whatever the type of the two transitions connecting these three states. Additionally, when the transition of type j is a simple wave, also the transition state T_j can prevail at steady state under the conditions specified in eqs 22 and 24. In general, at steady state, the composition is homogeneous along the column. However, when one of the transitions, say that of type 2, is a shock and it is standing, i.e., its propagation speed is zero, then at steady state, the column is occupied partly by one and partly by the other of the states separated by that transition, say states A and I. Nevertheless, the net flux of each species, which is given by $f_i = mc_i^{ss} - n_i^{ss}$, where ss refers to the steady state, is unambiguously defined since this expression yields the same quantity whatever the state across the standing shock is used to calculate it, as it can easily be checked.

It is worth noting that, knowing the steady state and using eq 5, the following useful expression for the dimensionless net flux of i in section j of a TMB unit defined in eq 4 can be obtained:

$$f_i^j = m_j c_{i,j}^{ss} - n_{i,j}^{ss} = (m_j\delta_j - H_i)c_{i,j}^{ss}/\delta_j \quad (i = 1, 2; j = 1, ..., 4) \tag{26}$$

On the basis of the attained steady state, the composition of the fluid stream from the right end of the column, c_i^b, and that of the solid stream from the left end of the column, n_i^a, are calculated through the following mass balances at the column ends:

$$(m + \eta)c_i^b = mc_i^{ss} - n_i^{ss} + n_i^b + \eta c_i^B \quad (i = 1, 2) \tag{27}$$

$$n_i^a + \eta c_i^a = (m + \eta)c_i^A + n_i^{ss} - mc_i^{ss} \quad (i = 1, 2) \tag{28}$$

where $\eta = \epsilon_p/(1 - \epsilon_p)$. The small superscripts used for c_i^b and n_i^a distinguish these concentrations from those at equilibrium with the inlet solid and fluid streams, i.e., n_i^B and c_i^A, which are indicated as c_i^B and n_i^A, respectively. It is worth noting that when the steady state coincides with one of the two inlet states, then the outlet stream from the same column end corresponds to the same state (see Appendix A.1).

The last two equations can be recast in terms of the function $F(\omega)$ defined by eq 8 in a rather effective and useful way. To this aim, one has to take eqs 89 and 90 of Appendix A into account, multiply the column end balances 27 and 28 by $p_i K_i/(H_i - \omega)$, sum over the index i, and then multiply by ω both sides of the resulting equation; this procedure yields the following two equations in ω, one for each column end:

$$\delta_b(m + \eta)(F^b(\omega) - 1) = (\omega + \eta\delta_B)(F^B(\omega) - 1) + (m\delta_{ss} - \omega)(F^{ss}(\omega) - 1) \tag{29}$$

$$(\omega + \eta\delta_a)(F^a(\omega) - 1) = \delta_A(m + \eta)(F^A(\omega) - 1) - (m\delta_{ss} - \omega)(F^{ss}(\omega) - 1) \tag{30}$$

Note that here the same convention as in the previous equations is adopted as to how superscripts are used to identify composition states; hence, $F^\alpha(\omega_i^\alpha) = 1$ for any state α.

Finally, it can be demonstrated that the ω_i values characterizing the composition states of the two outgoing fluid and solid streams and of the constant state inside the column attained at steady state fulfill the following constraints:

$$\min\{\omega_i^A,\omega_i^B\} \le \omega_i \le \max\{\omega_i^A,\omega_i^B\} \quad (i = 1, 2) \tag{31}$$

This property is a straightforward consequence of eqs 21−25 in the case of the state prevailing at steady state, whereas it is proven in Appendix A.2 for the case of the two outlet streams. Furthermore, if the constant state corresponding to the inlet stream at one end of the column and the one prevailing inside the column at steady state have one ω value in common, then that value is also one of those characterizing the outlet stream at the same end of the column (see Appendix A.1).

3. Complete Separation Conditions

Let us consider the four-section SMB unit in Figure 1, the equivalent TMB unit in Figure 2, and its binary operations where complete separation of the two solutes in the feed is achieved. The aim is to derive criteria on the operating parameters that can be applied to all the four generalized Langmuir isotherms considered in this work.

In the frame of the equilibrium theory model of chromatography, complete separation is achieved when the more retained component is collected only in the extract, and the less retained component, only in the raffinate, i.e., when $c_1^E = 0$ and $c_2^R = 0$. In other words, under complete separation conditions, 100% purity is achieved both in the extract with respect to the more retained component and in the raffinate with respect to the less retained component. In terms of ω values, this implies that H_1 and H_2 are one of the two values characterizing the extract and the raffinate, respectively.

It is worth noting that, in the TMB unit of Figure 2, the ω values characterizing any stream in the unit are constrained to be between the corresponding ones of the two inlet streams, i.e., the feed corresponding to (ω_1^F,ω_2^F) and the desorbent, which is assumed to be fully regenerated and is characterized by the pair (H_1, H_2). This means that

$$\min\{\omega_i^F, H_i\} \le \omega_i \le \max\{\omega_i^F, H_i\} \quad (i = 1, 2) \qquad (32)$$

and is a consequence of the results demonstrated in Appendix A.5. The last equation guarantees that if the feed mixture fulfills the constraints stated in section 2.2, namely, that requiring $\delta_F > 0$, and those of eq 7, then any state within the TMB units fulfills them too. The ultimate reason for that is the structure of the characteristic fields in the hodograph plane, as illustrated in Figure 1 of the earlier work.[18]

Requiring complete separation implies specifying the following properties on the net flow rates of each species in the four sections of the unit.

$$\text{section 1:} \quad f_1^1 = 0, \quad f_2^1 = 0 \qquad (33)$$

$$\text{section 2:} \quad f_1^2 = 0, \quad f_2^2 = -(m_3 - m_2)c_2^F \qquad (34)$$

$$\text{section 3:} \quad f_1^3 = (m_3 - m_2)c_1^F, \quad f_2^3 = 0 \qquad (35)$$

$$\text{section 4:} \quad f_1^4 = 0, \quad f_2^4 = 0 \qquad (36)$$

The conditions on f_2^2 and f_1^3 in eqs 34 and 35 express the requirement that component 1 be collected entirely in the raffinate and component 2 be collected entirely in the extract. The zero-flux conditions are a consequence of the constraints imposed on the steady states in the different TMB sections by the requirement that there be no leakage of the undesired component through the wrong column outlet. These constraints are derived in Appendix A.2 and, when applied to a four-section TMB unit, establish that, at steady state, component 1 can be present only in section 3, whereas component 2 can be present only in section 2 hence the zero values of the net flow rates f_i^j in all the other sections.

Equations 33−36 establish constraints on the possible composition states in the TMB unit, so strict that it is possible to define univocally the ω pairs characterizing all streams in the unit. These are shown in Figure 2; it is remarkable that the ω pairs are formally the same for all four generalized Langmuir isotherms. Note that the two streams before and after the feed node are labeled α and β, whereas the solid stream facing the feed node is labeled γ.

Some remarks to justify such conclusion are necessary. First, in principle, the extract stream could be characterized also by the vector (ω_1^E, H_1) in the case of the isotherm **L**, whereas the raffinate could be associated also to (H_2, ω_2^R) in case **A**; these pairs would fulfill in fact the general inequalities 9 and 10, respectively, as well as eqs 34 and 35. However, this choice would violate the constraints of eq 32; hence, it is not feasible, and the states in Figure 2 are the only ones to be considered in the following analysis.

Second, the steady states attained in sections 2 and 3 are the intermediate states as to the nomenclature defined in section 2.3. However, on the basis of the analysis in Appendix A.3, also the fluid state entering section 2, i.e., that of the extract stream, as well as the transition state between the extract state and the intermediate state for the isotherms where the corresponding transition is a simple wave (isotherms **L** and $\mathbf{M}_2$) would be allowed at steady state to guarantee 100% extract purity. Likewise, the solid state entering section 3 and the corresponding transition state when feasible (isotherms **A** and $\mathbf{M}_2$) would be admissible in section 3. However, the possible transition states do not add any additional operating point to the complete separation region determined by considering only the intermediate states as feasible steady states; this result is demonstrated in Appendix B.3. In turn, the property that the extract and the raffinate states cannot prevail in section 2 and 3, respectively, is demonstrated in Appendix B.2.

Finally, in Figure 2, already taken into account is the fact that $\omega_2^\alpha = \omega_2^\gamma$ and $\omega_1^\beta = \omega_1^\gamma$ because both ω_2^γ and ω_1^β are shared by an inlet stream and by the steady state in sections 2 and 3, respectively; hence, they are also associated to the outlet streams from the same column's end as demonstrated in Appendix A.1. This implies fulfilling the material balances of species 2 at the right end of section 2 and of species 1 at the left end of section 3.

The composition of all streams in Figure 2 can be determined once eight unknown ω values are determined; these are ω_1^α, ω_2^β, ω_1^γ, ω_2^γ, ω_2^E, ω_2^{ES}, ω_1^R, and ω_1^{RS}. These can be calculated for a given set of operating conditions, i.e., of flow rate ratios m_j (j = 1, ..., 4), by solving eight independent equations, namely, the overall material balances for both components, together with the material balances of the less retained component 1 at the left end of section 4, at the right end of section 3, and at the right end of section 2 and those of the more retained component 2 at the right end of section 1, at the left end of section 2, and at the left end of section 3, where the fluid and adsorbed phase concentrations are written using the inverse relationships 13−17. Straightforward overall balances are used to express the external flow rates of desorbent, feed, extract, and raffinate in terms of flow rate ratios, thus yielding the following eight equations:

$$(m_3 - m_4)c_1^R = (m_3 - m_2)c_1^F \quad (37)$$

$$(m_1 - m_2)c_2^E = (m_3 - m_2)c_2^F \quad (38)$$

$$n_1^{RS} + \eta c_1^{RS} = (m_3 + \eta)c_1^R \quad (39)$$

$$(m_3 + \eta)c_1^R = m_3 c_1^3 - n_1^3 + n_1^{RS} + \eta c_1^{RS} \quad (40)$$

$$n_1^\gamma + \eta c_1^\gamma = (m_2 + \eta)c_1^\alpha \quad (41)$$

$$n_2^{ES} + \eta c_2^{ES} = (m_1 + \eta)c_2^E \quad (42)$$

$$n_2^{ES} + \eta c_2^{ES} = (m_2 + \eta)c_2^E - (m_2 c_2^2 - n_2^2) \quad (43)$$

$$n_2^\gamma + \eta c_2^\gamma = (m_3 + \eta)c_2^\beta \quad (44)$$

It is worth noting that the complete separation conditions on f_1^3 and f_2^2 in eqs 35 and 34 are linear combinations of the material balances on components 1 and 2, respectively. Equations 40 and 43 can be replaced by these linear combinations, which can be recast as

$$(m_3 - m_2)c_1^F = m_3 c_1^3 - n_1^3 \quad (45)$$

$$(m_3 - m_2)c_2^F = -(m_2 c_2^2 - n_2^2) \quad (46)$$

These two equations are remarkably convenient; expressing the concentrations on their right-hand side (rhs) in terms of the relevant ω values yields in fact the following two quadratic equations in a single unknown, namely, ω_1^γ and ω_2^γ, respectively:

$$f_1(\omega_1^\gamma) = (\omega_1^\gamma)^2 - B_1\omega_1^\gamma + C_1 = 0 \quad (47)$$

$$f_2(\omega_2^\gamma) = (\omega_2^\gamma)^2 - B_2\omega_2^\gamma + C_2 = 0 \quad (48)$$

where

$$B_1 = m_3 + H_1 + p_1 K_1 c_1^F (m_3 - m_2) \quad (49)$$

$$C_1 = m_3 H_1 \quad (50)$$

$$B_2 = m_2 + H_2 - p_2 K_2 c_2^F (m_3 - m_2) \quad (51)$$

$$C_2 = m_2 H_2 \quad (52)$$

Necessary conditions for a pair of values of m_2 and m_3 to be feasible are that the two quadratic equations above have real roots, which is guaranteed by the two conditions:

$$B_1^2 - 4C_1 \geq 0 \quad (53)$$

$$B_2^2 - 4C_2 \geq 0 \quad (54)$$

The two roots of eq 47 will be called $\omega_1^\ominus$ and $\omega_1^\oplus$, with $\omega_1^\ominus \leq \omega_1^\oplus$, and those of eq 48 will be accordingly named $\omega_2^\ominus$ and $\omega_2^\oplus$. Only one of the two solutions equals ω_1^γ or ω_2^γ, whereas the other has to be discarded.

It is also worth recasting eq 44 in terms of ω values instead of concentrations, thus yielding

$$\omega_2^\beta(H_2 - \omega_2^\gamma)(\omega_1^\gamma\omega_2^\gamma + \eta H_1) = H_1\omega_2^\gamma(H_2 - \omega_2^\beta)(m_3 + \eta) \quad (55)$$

Once a set of m_j values is assigned to specify the TMB operation of interest, then the equations above can be solved and the composition state of all TMB streams can be determined. This can be done sequentially, by solving first eqs 47, 48, 37, and 38 for ω_1^γ, ω_2^γ, ω_1^R, and ω_2^E, respectively, and then eqs 39, 42, 41, and 44 for ω_1^{RS}, ω_2^{ES}, ω_1^α, and ω_2^β, respectively. It is worth noting that ω_1^γ, ω_2^γ, ω_1^α, and ω_2^β depend only on m_2 and m_3, whereas the other four ω values depend also on either m_1 or m_4.

However, not any choice of the flow rate ratios is feasible, since the material balance equations are written under the complete separation assumption, which poses constraints on the flow rate ratios themselves. In other words, the material balance equations above apply if and only if the states shown in Figure 2 are indeed attained at steady state, which occurs only if the constraints on the flow rate ratios derived from the general ones stated in eqs 21−25 and reported in Table 1 are fulfilled. The inequalities in Table 1 are written after considering the values ω_1 and ω_2 associated to the fluid and the solid stream entering each TMB section and establishing which is the larger. This is easy wherever the pair of ω values to be compared includes also H_1 and H_2, since one can exploit eqs 9−12 and 32, but it is more complicated in the other cases, namely, for ω_1^γ and ω_1^{RS} and for ω_2^γ and ω_2^E. Such assessment is carried out in Appendix B.1 and leads to the conclusion that the determination of which of the ω values is larger in the two pairs above depends on the specific adsorption isotherm: in particular, on one hand, $\omega_1^{RS} > \omega_1^\gamma$ in cases **L** and $\mathbf{M}_1$, whereas $\omega_1^{RS} < \omega_1^\gamma$ in cases **A** and $\mathbf{M}_2$; on the other hand, $\omega_2^E > \omega_2^\gamma$ in cases **L** and $\mathbf{M}_2$, whereas $\omega_2^E < \omega_2^\gamma$ in cases **A** and $\mathbf{M}_1$.

The constraints in Table 1 are implicit with respect to the flow rate ratios. The objective of the next sections is to transform them into explicit constraints that define the complete separation region in the space of the operating parameters. Operating points in this region are characterized by flow rate ratios m_j that fulfill also the obvious requirement that the external flow rates in the TMB and SMB units be positive, i.e., that $m_1 > m_2$, $m_2 < m_3$, $m_3 > m_4$, and $m_4 < m_1$.

3.1. Complete Separation Conditions in the (m_2, m_3) Plane. Let us first consider sections 2 and 3 of the TMB unit and the corresponding constraints reported in Table 1. In all four cases, the lower bounds on $m_2\delta_2$ and the upper bounds on $m_3\delta_3$ are given by parameters that are either constant (H_1 and H_2) or a function of only m_2 and m_3 (ω_1^γ and ω_2^β; see the discussion in the previous section). The other two parameters defining the lower bound for section 3 and the upper bound for section 2, i.e., ω_1^{RS} and ω_2^E, depend also on m_4 and m_1, respectively. It is also worth noting that using eq 15 and considering the steady states in sections 2 and 3 shown in Figure 2 yields $\delta_2 = H_2/\omega_2^\gamma$ and $\delta_3 = H_1/\omega_1^\gamma$. Moreover, the two real roots of eqs 47 and 48 fulfill the relationships $\omega_1^\ominus\omega_1^\oplus = m_3H_1$ and $\omega_2^\ominus\omega_2^\oplus = m_2H_2$. Combining these two observations demonstrates that $m_2\delta_2$ equals the root of eq 48 that is not ω_2^γ and, accordingly, that $m_3\delta_3$ takes the value of the root of eq 47 that is not ω_1^γ.

Let us now consider the complete separation constraints for each individual isotherm separately.

3.1.1. Langmuir Isotherm, Case L. On the basis of the observations above, the constraints on $m_2\delta_2$ and $m_3\delta_3$ in Table 1 can be recast as constraints on the relevant ω values:

$$H_1 \leq \frac{\omega_2^\ominus\omega_2^\oplus}{\omega_2^\gamma} \leq \omega_2^\gamma \quad (56)$$

$$\omega_1^{RS} \leq \frac{\omega_1^\ominus\omega_1^\oplus}{\omega_1^\gamma} \leq \omega_2^\beta \quad (57)$$

Table 1. Constraints on the Operating Conditions in Sections 1−4 of the TMB Unit to Achieve Complete Separation

isotherm	section 1	section 2	section 3	section 4
L	$H_2 \le m_1\delta_1$	$H_1 \le m_2\delta_2 \le \omega_2^{\gamma}$	$\omega_1^{RS} \le m_3\delta_3 \le \omega_2^{\beta}$	$m_4\delta_4 \le \omega_1^{R}$
A	$\omega_2^{ES} \le m_1\delta_1$	$\omega_1^{\gamma} \le m_2\delta_2 \le \omega_2^{E}$	$\omega_1^{\gamma} \le m_3\delta_3 \le H_2$	$m_4\delta_4 \le H_1$
$\mathbf{M}_1$	$\omega_2^{ES} \le m_1\delta_1$	$H_1 \le m_2\delta_2 \le \omega_2^{E}$	$\omega_1^{RS} \le m_3\delta_3 \le H_2$	$m_4\delta_4 \le \omega_1^{R}$
$\mathbf{M}_2$	$H_2 \le m_1\delta_1$	$\omega_1^{\gamma} \le m_2\delta_2 \le \omega_2^{\gamma}$	$\omega_1^{\gamma} \le m_3\delta_3 \le \omega_2^{\beta}$	$m_4\delta_4 \le H_1$

Table 2. Complete Separation Constraints on the Operating Conditions in Sections 1−4 of the TMB Unit Expressed in Terms of Feasible Ranges of the Roots of Equations 47 and 48

isotherm	$\omega_1^{\gamma} = \omega_1^{\ominus}$	$\omega_2^{\gamma} = \omega_2^{\oplus}$	section 1	section 2	section 3	section 4
L	$\omega_1^{F} \le \omega_1^{\ominus} \le H_1$	$\omega_2^{F} \le \omega_2^{\oplus} \le H_2$	$m_1 \ge H_2$	$H_1 \le \omega_2^{\ominus} \le \omega_2^{\oplus}$	$\omega_1^{\oplus} \le \omega_2^{\oplus}$	$m_4 \le \omega_1^{\ominus}$
A	$H_1 \le \omega_1^{\ominus} \le \omega_1^{F}$	$H_2 \le \omega_2^{\oplus} \le \omega_2^{F}$	$m_1 \ge \omega_2^{\oplus}$	$\omega_1^{\ominus} \le \omega_2^{\ominus}$	$\omega_1^{\ominus} \le \omega_1^{\oplus} \le H_2$	$m_4 \le H_1$
$\mathbf{M}_1$	$\omega_1^{F} \le \omega_1^{\ominus} \le H_1$	$H_2 \le \omega_2^{\oplus} \le \omega_2^{F}$	$m_1 \ge \omega_2^{\oplus}$	$H_1 \le \omega_2^{\ominus}$	$\omega_1^{\oplus} \le H_2$	$m_4 \le \omega_1^{\ominus}$
$\mathbf{M}_2$	$H_1 \le \omega_1^{\ominus} \le \omega_1^{F}$	$\omega_2^{F} \le \omega_2^{\oplus} \le H_2$	$m_1 \ge H_2$	$\omega_1^{\ominus} \le \omega_2^{\ominus} \le \omega_2^{\oplus}$	$\omega_1^{\ominus} \le \omega_1^{\oplus} \le \omega_2^{\oplus}$	$m_4 \le H_1$

Note that the former equation can be fulfilled if and only if

$$\omega_2^{\gamma} = \omega_2^{\oplus} \tag{58}$$

which forces the right inequality in eq 56 to be fulfilled provided condition 54 holds. Moreover, from eq 47, $f_1(\omega)$ is a convex parabola; hence, $\omega_1^{\ominus} < H_1 < \omega_1^{\oplus}$ since $f_1(H_1) < 0$. From eq 9, it follows that

$$\omega_1^{\gamma} = \omega_1^{\ominus} \tag{59}$$

and that the left inequality in eq 57 is always fulfilled because $\omega_1^{RS} \le H_1$ by definition. The right inequality in the same equation reduces then to $\omega_1^{\oplus} \le \omega_2^{\beta}$, which by using eq 55 can easily be proved to be equivalent to $\omega_1^{\oplus} \le \omega_2^{\gamma}$. Therefore, it can be concluded that the complete separation constraints on the flow rate ratios in sections 2 and 3 reduce to the following inequalities on the roots of eqs 47 and 48:

$$H_1 \le \omega_2^{\ominus} \le \omega_2^{\oplus} \tag{60}$$

$$\omega_1^{\oplus} \le \omega_2^{\oplus} \tag{61}$$

The parameters ω_1^{γ} and ω_2^{γ} have also to fulfill constraints 32, which are a consequence of the coupling between the different sections of the TMB unit. These results are summarized in Table 2.

3.1.2. Anti-Langmuir Isotherm, Case A. Similarly to case **L**, the constraints on $m_2\delta_2$ and $m_3\delta_3$ in Table 1 can be recast as follows:

$$\omega_1^{\gamma} \le \frac{\omega_2^{\ominus}\omega_2^{\oplus}}{\omega_2^{\gamma}} \le \omega_2^{E} \tag{62}$$

$$\omega_1^{\gamma} \le \frac{\omega_1^{\ominus}\omega_1^{\oplus}}{\omega_1^{\gamma}} \le H_2 \tag{63}$$

The second equation holds only if $\omega_1^{\gamma} = \omega_1^{\ominus}$. According to eq 48, $f_2(\omega)$ is also a convex parabola and $f_2(H_2) < 0$; therefore, $\omega_2^{\ominus} < H_2 < \omega_2^{\oplus}$, eq 10 leads to $\omega_2^{\gamma} = \omega_2^{\oplus}$, and the right inequality of eq 62 is trivially fulfilled as $\omega_2^{E} \ge H_2$ due again to eq 10. Therefore, the complete separation constraints for sections 2 and 3 are as follows (see Table 2, where also those stemming from eq 32 are reported):

$$\omega_1^{\ominus} \le \omega_2^{\ominus} \tag{64}$$

$$\omega_1^{\ominus} \le \omega_1^{\oplus} \le H_2 \tag{65}$$

The left inequality of eq 65 requires that eq 53 be fulfilled.

3.1.3. Mixed Langmuir Isotherm, Case $\mathbf{M}_1$. The constraints reported in Table 1 are a different combination of those considered in the two previous cases and, also, in this case $f_1(H_1) < 0$ and $f_2(H_2) < 0$. Following similar arguments leads again to $\omega_1^{\gamma} = \omega_1^{\ominus}$ and to $\omega_2^{\gamma} = \omega_2^{\oplus}$, as well as to the following constraints (see also Table 2):

$$H_1 \le \omega_2^{\ominus} \tag{66}$$

$$\omega_1^{\oplus} \le H_2 \tag{67}$$

Note that, in this case, both eqs 53 and 54 hold true always.

3.1.4. Mixed Langmuir Isotherm, Case $\mathbf{M}_2$. On the basis of similar arguments as above, it is rather straightforward from the constraints in Table 1 to arrive at the conclusion that $\omega_1^{\gamma} = \omega_1^{\ominus}$ and $\omega_2^{\gamma} = \omega_2^{\oplus}$ also in this case and that complete separation requires that (see, also, Table 2)

$$\omega_1^{\ominus} \le \omega_2^{\ominus} \le \omega_2^{\oplus} \tag{68}$$

$$\omega_1^{\ominus} \le \omega_1^{\oplus} \le \omega_2^{\oplus} \tag{69}$$

The right inequality of eq 68 and the left one of eq 69 are fulfilled if both eqs 53 and 54 hold true.

3.2. Complete Separation Conditions on m_1 and m_4. The constraints on the flow rate ratios in sections 1 and 4 to achieve complete separation that are reported in Table 1 can all be simplified by noting that at steady state both sections are saturated with pure solvent; hence, $\delta_1 = \delta_4 = 1$. Moreover, some of the constraints are explicit and independent of the flow rates in sections 2 and 3, whereas others involve ω_1^{R} and ω_2^{ES} that are to be determined as a function of the other flow rate ratios through the material balance eqs 37−44. Substituting such results into the constraints on m_1 and m_4 yields inequalities with a lower and an upper bound on m_1 and m_4, respectively, which depend on m_2 and m_3.

First, let us consider the overall balance for component 1, i.e., eq 37, which can be solved for ω_1^{R}, thus yielding

$$\frac{H_1}{\omega_1^{R}} = 1 + \frac{m_3 - m_2}{m_3 - m_4} K_1 c_1^{F} \tag{70}$$

Substituting this into the constraint $m_4 \le \omega_1^{R}$ that applies to cases **L** and $\mathbf{M}_1$ leads to the inequality:

$$m_4^{\,2} - B_1 m_4 + C_1 \ge 0 \tag{71}$$

where B_1 and C_1 are given by eqs 49 and 50. The corresponding

equation, which is the same as eq 47, has roots $\omega_1^{\ominus}$ and $\omega_1^{\oplus}$, of which only the first is smaller than H_1 as ω_1^{R} also is. Hence, as reported also in Table 2, the final constraint on m_4 is

$$m_4 \le \omega_1^{\ominus} \tag{72}$$

In cases **A** and $\mathbf{M}_1$, eqs 38 and 42 have to be used first to obtain the following quadratic equation for ω_2^{ES}:

$$(m_1 - m_2)(\omega_2^{ES})^2 + \omega_2^{ES}[(m_1 - m_2)(\eta - H_2) - (m_1 + \eta)(m_3 - m_2)K_2c_2^F] - (m_1 - m_2)\eta H_2 = 0 \tag{73}$$

which has a positive and a negative root. The constraint $m_1 \ge \omega_2^{ES}$ is equivalent to requiring that the left-hand side of the last equation be nonnegative when calculated for $\omega_2^{ES} = m_1$; this leads to the following cubic inequality in m_1:

$$(m_1 + \eta)({m_1}^2 - B_2m_1 + C_2) \ge 0, \tag{74}$$

where B_2 and C_2 are given by eqs 51 and 52. This is fulfilled when $m_1 > -\eta$, which due to eq 3 is tantamount to saying that $Q_1^{TMB} > 0$, if the second factor in the left-hand side is nonnegative, i.e., when m_1 is larger than the larger of the roots of eq 48:

$$m_1 \ge \omega_2^{\oplus} \tag{75}$$

as reported also in Table 2.

4. Region of Complete Separation in the Operating Parameter Space

In this chapter, the complete separation conditions derived above and reported in Table 2 will be transformed into explicit constraints, to obtain a complete separation region in the operating parameters space, whose coordinates are the flow rate ratios m_j ($j = 1, ..., 4$). The projection of the four dimension domain onto the (m_2, m_3) will be shown to be independent of m_1 and m_4 and to apply provided these fulfill their corresponding constraints to achieve complete separation. An effective graphical representation of such projection will be provided.

4.1. Explicit Constraints on m_1 and m_4. With reference to Table 2, the constraints on m_1 and m_4 are in some cases explicit, but in others, they are expressed in terms of solutions of eqs 47 and 48. It can be readily observed that in both cases, where m_1 cannot be larger than $\omega_2^{\oplus}$, p_2 equals -1; hence, $B_2 > 0$ from eq 51. It follows that the relevant constraint on m_1 is given by

$$\text{Cases } \mathbf{A} \text{ and } \mathbf{M}_1\text{: } m_1 \ge m_{1,cr}(m_2, m_3, c_2^F) = \omega_2^{\oplus} = \frac{1}{2}\{m_2 + H_2 - p_2K_2c_2^F(m_3 - m_2) + \sqrt{[m_2 + H_2 - p_2K_2c_2^F(m_3 - m_2)]^2 - 4m_2H_2}\} \tag{76}$$

Likewise, in both cases, where m_4 has to be smaller or equal to $\omega_1^{\ominus}$, the conditions $p_1 = 1$ and $B_1 > 0$ hold and the constraint on m_4 can be recast in the following explicit form:

$$\text{Cases } \mathbf{L} \text{ and } \mathbf{M}_1\text{: } m_4 \le m_{4,cr}(m_2, m_3, c_1^F) = \omega_1^{\ominus} = \frac{1}{2}\{m_3 + H_1 + p_1K_1c_1^F(m_3 - m_2) - \sqrt{[m_3 + H_1 + p_1K_1c_1^F(m_3 - m_2)]^2 - 4m_3H_1}\} \tag{77}$$

It is worth noting that the lower and upper bounds in the previous inequalities, which are function of the operating point in the (m_2, m_3) plane and of the feed composition, are always more restrictive than the constant bounds that apply to the other cases according to Table 2, i.e.

$$\text{Cases } \mathbf{L} \text{ and } \mathbf{M}_2\text{: } m_1 \ge m_{1,cr} = H_2 \tag{78}$$

$$\text{Cases } \mathbf{A} \text{ and } \mathbf{M}_2\text{: } m_4 \le m_{4,cr} = H_1 \tag{79}$$

4.2. Complete Separation Region in the (m_2, m_3) Plane. It can be readily observed that all constraints associated to sections 2 and 3 of the TMB unit reported in Table 2 are independent of m_1 and m_4, since they involve only roots of eqs 47 and 48 where the only flow rates ratios that appear are m_2 and m_3. Therefore, it is possible to determine the geometric representation of the projection of the four-dimensional complete separation region onto the plane (m_2, m_3), i.e., what will be called in the following simply the complete separation region. This is a two-dimensional region of the plane, which is bounded by a number of straight lines and curves, which differ for the four different isotherms. The relationships defining such boundaries are summarized in Table 3. The coordinates of the intersection points of such lines can also be given compact relations, which are reported in Table 4. The notation used for lines and points in the text, tables, and accompanying figures is self-explanatory. Finally, Table 5 summarizes which lines, i.e., which boundaries, apply to the complete separation region for each of the four generalized Langmuir isotherms that will be analyzed in the following separately.

4.2.1. Mixed Langmuir Isotherm, Case $\mathbf{M}_1$. With reference to Table 2, for this isotherm, there are six constraints on the roots of eqs 47 and 48 that have to be fulfilled. Each of them is to be analyzed either to turn it into an explicit relationship in the (m_2, m_3) plane or to discard it because it is automatically fulfilled. The points in the (m_2, m_3) plane that fulfill all the remaining inequalities after this selection constitute the complete separation region, which is drawn in Figure 4.

Let us consider the constraint associated to section 2, i.e., $H_1 \le \omega_2^{\ominus}$. Since the function $f_2(\omega)$ defined by eq 48 is a convex parabola, the constraint is fulfilled if and only if the following relationship holds:

$$f_2(H_1) = {H_1}^2 - B_2H_1 + C_2 \ge 0 \tag{80}$$

Substituting eqs 51 and 52 allows expressing this inequality in terms of m_2 and m_3 and obtaining the equation of the straight line **bw**, which is reported in Table 3 and drawn in Figure 4. The equation of the line depends on the adsorption isotherm parameters as well as on the feed concentration of the more retained component. In all cases, it goes through point **b** of coordinates (H_1, H_1) (see Table 4).

The constraint $\omega_1^{\oplus} \le H_2$, which is associated to section 3, can be treated similarly, being that $f_1(\omega)$ is also a convex parabola; this leads to the following relationship:

$$f_1(H_2) = {H_2}^2 - B_1H_2 + C_1 \ge 0 \tag{81}$$

Substituting eqs 49 and 50 yields an inequality in terms of m_2 and m_3, which depends also on the adsorption isotherm parameters and on the feed concentration of the less retained species. This defines the straight line **aw** that passes always through point **a** and whose equation is given in Table 3.

The right constraint on $\omega_1^{\ominus}$ in Table 2 can be recast as $f_1(H_1) \ge 0$. With reference to eq 47, it can readily be seen that $f_1(H_1)$

Table 3. Straight Lines and Curves that Form the Boundaries of the Complete Separation Regions in the (m_2, m_3) Plane

line	equation	isotherms	refs
ab	$m_3 = m_2$	**L**, **A**, $\mathbf{M}_1$, $\mathbf{M}_2$	eq 82
ar	$m_3 = m_2 + (\sqrt{m_2} - \sqrt{H_2})^2/(p_2K_2c_2^F)$	**L**, $\mathbf{M}_2$	eq 85
aw	$m_3[H_2(1 + p_1K_1c_1^F) - H_1] - p_1K_1c_1^FH_2m_2 = H_2(H_2 - H_1)$	**A**, $\mathbf{M}_1$	eq 81
rw	$m_2H_2(\omega_1^F - H_1) + m_3H_1(H_2 - \omega_1^F) = \omega_1^F\omega_2^F(H_2 - H_1)$	**L**, $\mathbf{M}_2$	eq 86
bs	$m_2 = m_3 + (\sqrt{m_3} - \sqrt{H_1})^2/(p_1K_1c_1^F)$	**A**, $\mathbf{M}_2$	eq 87
sw	$m_2H_2(\omega_2^F - H_1) + m_3H_1(H_2 - \omega_2^F) = \omega_1^F\omega_2^F(H_2 - H_1)$	**A**, $\mathbf{M}_2$	eq 88
bw	$p_2K_2c_2^FH_1m_3 + m_2[H_2 - H_1(1 + p_2K_2c_2^F)] = H_1(H_2 - H_1)$	**L**, $\mathbf{M}_1$	eq 80

Table 4. Characteristic Points on the Boundary of the Complete Separation Regions in the (m_2, m_3) Plane[a]

point	m_2	m_3
a	H_2	H_2
b	H_1	H_1
f	ω_2^F	ω_2^F
g	ω_1^F	ω_1^F
r	$(\omega_2^F)^2/H_2$	$\{\omega_2^F[\omega_2^F(H_1 - \omega_1^F) + \omega_1^F(H_2 - H_1)]\}/H_1(H_2 - \omega_1^F)$
s	$\{\omega_1^F[\omega_1^F(\omega_2^F - H_2) + \omega_2^F(H_2 - H_1)]\}/H_2(\omega_2^F - H_1)$	$(\omega_1^F)^2/H_1$
$\mathbf{w}_\mathbf{L}$ (case **L**)	$\omega_2^FH_1/H_2$	$\{\omega_2^F[H_1(H_1 - \omega_1^F) + \omega_1^F(H_2 - H_1)]\}/H_1(H_2 - \omega_1^F)$
$\mathbf{w}_\mathbf{A}$ (case **A**)	$\{\omega_1^F[H_2(\omega_2^F - H_2) + \omega_2^F(H_2 - H_1)]\}/H_2(\omega_2^F - H_1)$	$\omega_1^FH_2/H_1$
$\mathbf{w}_{\mathbf{M}_1}$ (case $\mathbf{M}_1$)	$H_1\{1 + [(H_2 - \omega_1^F)(\omega_2^F - H_2)(H_2 - H_1)]/ H_2[(H_1 - \omega_1^F)(\omega_2^F - H_2) + (H_2 - \omega_1^F)(\omega_2^F - H_1)]\}$	$H_2\{1 - [(H_1 - \omega_1^F)(\omega_2^F - H_1)(H_2 - H_1)]/ H_1[(H_1 - \omega_1^F)(\omega_2^F - H_2) + (H_2 - \omega_1^F)(\omega_2^F - H_1)]\}$
$\mathbf{w}_{\mathbf{M}_2}$ (case $\mathbf{M}_2$)	$\omega_1^F\omega_2^F/H_2 = H_1/\delta_F$	$\omega_1^F\omega_2^F/H_1 = H_2/\delta_F$

[a] The coordinates of each point are defined by the intersection of a pair of lines in Table 3.

Table 5. Summary Table Indicating Which Lines Constitute the Boundary of the Complete Separation Region in the (m_2, m_3) Plane for Different Isotherms[a]

	line						
isotherm	**ab**	**ar**	**rw**	**aw**	**bs**	**sw**	**bw**
L	√	√	√				√
A	√			√	√	√	
$\mathbf{M}_1$	√			√			√
$\mathbf{M}_2$	√	√	√		√	√	

[a] This table is based on Table 3.

is always negative but along the diagonal

$$m_3 = m_2 \tag{82}$$

meaning that the constraint under consideration is always fulfilled for nonnegative feed flow rates. The line of the last equation is called line **ab** and is obtained in a similar way also when the left constraint on $\omega_2^\oplus$ in Table 2 is considered, since $f_2(H_2) \leq 0$.

Now, let us consider the inequality $\omega_1^F \leq \omega_1^\ominus$ that originates from eq 32, which defines the attainable ranges of ω values by considering all possible material balances in the TMB unit. This observation explains why material balance considerations can be exploited also here to show that this inequality is automatically fulfilled provided that one among the constraints that have already been considered, namely, $H_1 \leq \omega_2^\ominus$, is fulfilled. To this aim, consider the material balance at the right end of section 2 (see Figure 2) written in the form of eq 29 and calculate the corresponding expression for $\omega = \omega_1^\ominus$, i.e.

$$\delta_\alpha(m_2 + \eta)(F^\alpha(\omega_1^\ominus) - 1) = (\omega_1^\ominus + \eta\delta_\gamma)(F^\gamma(\omega_1^\ominus) - 1) + (m_2\delta_2 - \omega_1^\ominus)(F^2(\omega_1^\ominus) - 1) \tag{83}$$

Since $\omega_1^\ominus$ is one of the ω values associated to the γ state, the first of the two addenda in the right-hand side is zero. The second factor in the second addendum in the right-hand side is negative, because component 1 is missing from the steady state in section 2 and according to its definition (eq 8) $F_2(\omega)$ is always negative where $\omega < H_2$ in case $\mathbf{M}_1$. On the other hand, the other factor, namely, $(m_2\delta_2 - \omega_1^\ominus)$, can be written as $(\omega_2^\ominus - \omega_1^\ominus)$ and is always positive, thanks to the inequalities $\omega_1^\ominus < H_1$ and $H_1 \leq \omega_2^\ominus$ that have already been considered and certainly apply. It follows that the left-hand side of eq 83 is negative; hence, $\omega_1^\ominus$ is smaller than ω_1^α, i.e., the root of equation $F^\alpha(\omega) = 1$, since $F(\omega)$ is monotonically increasing for $\omega < H_1$ in case $\mathbf{M}_1$. Considering that the feed stream and the α stream mix to yield the β stream, applying the results of Appendix A.4, and considering that $\omega_1^\beta = \omega_1^\ominus$ (see Figure 2) leads to the conclusion that $\omega_1^F < \omega_1^\ominus < \omega_1^\alpha$, whose left inequality is the one that was to be demonstrated.

The last constraint in Table 2, i.e., $\omega_2^\oplus \leq \omega_2^F$, can be shown to be fulfilled because $\omega_1^\oplus \leq H_2$ by considering the material

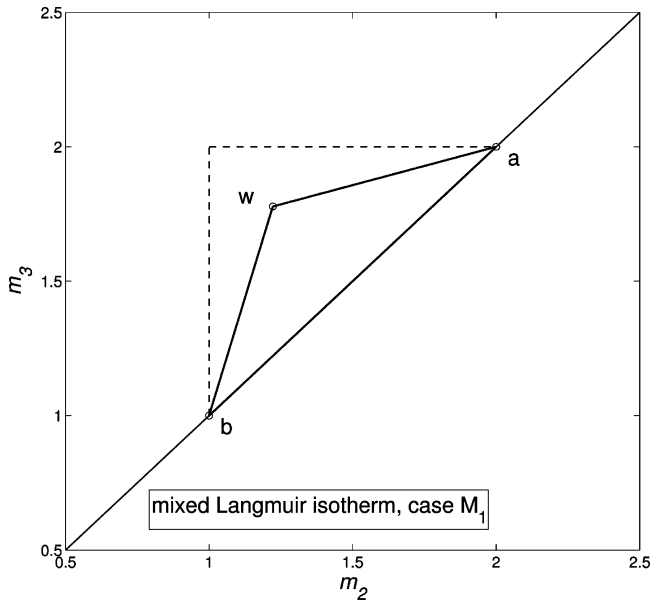

Figure 4. Region of complete separation in the (m_2, m_3) plane for the mixed Langmuir isotherm, case $\mathbf{M}_1$. The parameters are as follows: $H_1 = 1$, $H_2 = 2$, $K_1 = 0.1$ L/g, $K_2 = 0.2$ L/g, $c_1^F = c_2^F = 2$ g/L. The dashed lines define the linear complete separation region.

balance at the left end of section 3 in the form of eq 30 where $\omega = \omega_2^{\beta}$, i.e., the following relationship:

$$(\omega_2^{\beta} + \eta\delta_{\gamma})(F^{\gamma}(\omega_2^{\beta}) - 1) = \delta_{\beta}(m_3 + \eta)(F^{\beta}(\omega_2^{\beta}) - 1) - (m_3\delta_3 - \omega_2^{\beta})(F^3(\omega_2^{\beta}) - 1) \quad (84)$$

The first term in the right-hand side is zero by definition. The second factor of the second addendum on the right-hand side is negative, since with no component 1 in section 3 the function $F^3(\omega)$ is always negative for $\omega > H_1$ in case $\mathbf{M}_1$. Finally, $(m_3\delta_3 - \omega_2^{\beta}) = (\omega_1^{\oplus} - \omega_2^{\beta}) < 0$, since $\omega_1^{\oplus} \le H_2$ and $H_2 \le \omega_2^{\beta}$. It follows that $(F^{\gamma}(\omega_2^{\beta}) - 1) < 0$ and $\omega_2^{\alpha} = \omega_2^{\oplus} < \omega_2^{\beta}$; finally, by considering the feed node of the TMB unit and the results of Appendix A.4, one concludes that $\omega_2^{\oplus} < \omega_2^{\beta} < \omega_2^{\mathrm{F}}$, which is the result to be proved.

Thus concluding, the boundary of the complete separation region in the (m_2, m_3) plane for the mixed Langmuir isotherm $\mathbf{M}_1$ consists of three straight segments, i.e., lines **ab**, **bw**, and **aw**, as shown in Figure 4 and in Table 5. The intersection of lines **bw** and **aw** is the point $\mathbf{w}_{\mathrm{M1}}$, whose coordinates can be obtained in a straightforward manner and are reported in Table 4; it can be readily observed that $m_{2,\mathrm{w}} \ge H_1$ and $m_{3,\mathrm{w}} \le H_2$. The vertex of the complete separation region is the point at the maximum distance from the diagonal, thus leading to the maximum theoretical productivity of the process.[8]

4.2.2. Langmuir Isotherm, Case L. Table 2 reports seven constraints for the Langmuir isotherm. It is straightforward to show that four of them are the same as those of case $\mathbf{M}_1$ and lead to the same conclusions. More specifically, $H_1 \le \omega_2^{\ominus}$ associated to section 2 leads to eq 80 and to line **bw** in Table 3; $\omega_1^{\mathrm{F}} \le \omega_1^{\ominus}$ is automatically fulfilled when the previous inequality holds true; $\omega_1^{\ominus} \le H_1$ and $\omega_2^{\oplus} \le H_2$ lead both to $m_3 \ge m_2$ and line **ab** as part of the boundary.

Let us consider the right inequality in the constraint associated to section 2, which expresses the requirement that eq 48 have real roots, i.e., that eq 54 be fulfilled. Note that this is not always the case as for the mixed Langmuir isotherm $\mathbf{M}_1$ since in the Langmuir case $f_2(H_2) > 0$ unless $m_3 = m_2$. Due to elementary properties of quadratic equations, the roots $\omega_2^{\ominus}$ and $\omega_2^{\oplus}$ have the same sign since C_2 is positive; $\omega_2^{\oplus}$ is positive because of eq 9; hence, both roots are positive, and so is B_2. On the basis of these observations, inequality 54 is equivalent to

$$B_2 \ge 2\sqrt{C_2} \ge 0 \quad (85)$$

which is fulfilled for all points below the curve **ar** in Table 3. This equation defines a parabola in the (m_2, m_3) plane that belongs to the half plane $m_3 \ge m_2$ and is tangent to the diagonal $m_3 = m_2$ in point **a** of coordinates (H_2, H_2).

Now, let us consider the lower bound on $\omega_2^{\oplus}$, i.e., $\omega_2^{\mathrm{F}} \le \omega_2^{\oplus}$. Trying to repeat the argument used for case $\mathbf{M}_1$ in order to prove that this inequality is always fulfilled would not work, because in the Langmuir case the inequality $\omega_1^{\oplus} \le H_2$ does not hold. It follows that, due to the convexity of $f_2(\omega)$, $\omega_2^{\mathrm{F}} \le \omega_2^{\oplus}$ requires that

$$f_2(\omega_2^{\mathrm{F}}) = (\omega_2^{\mathrm{F}})^2 - B_2\omega_2^{\mathrm{F}} + C_2 \le 0 \quad (86)$$

This inequality is fulfilled by points below the line **rw**, whose equation is given in Table 3 and is obtained by substituting eq 14 into eq 86. This straight line crosses the diagonal in point **f** of coordinates (ω_2^{F},ω_2^{F}), intersects the straight line **bw** in the optimal point $\mathbf{w}_{\mathrm{L}}$, and is tangent to line **ar** in point **r** (the coordinates of these points are reported in Table 4).

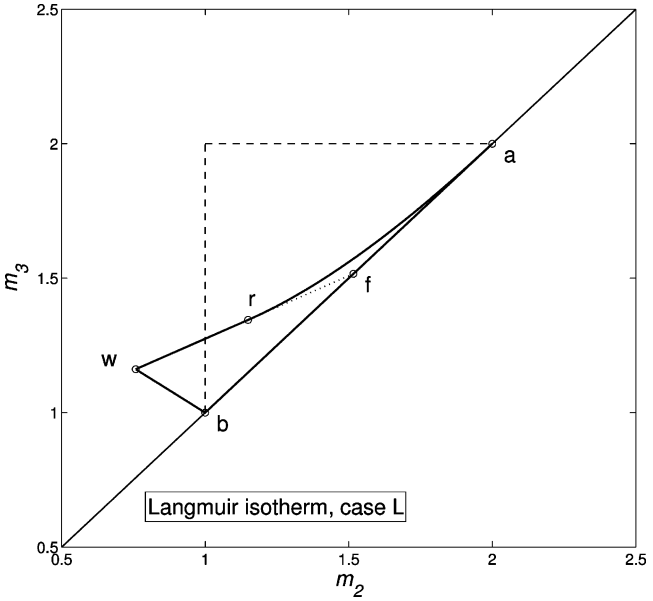

Figure 5. Region of complete separation in the (m_2, m_3) plane for the Langmuir isotherm, case **L**. The parameters are as follows: $H_1 = 1$, $H_2 = 2$, $K_1 = 0.1$ L/g, $K_2 = 0.2$ L/g, $c_1^{\mathrm{F}} = c_2^{\mathrm{F}} = 3$ g/L. The dashed lines define the linear complete separation region.

Finally, consider the constraint $\omega_1^{\oplus} \le \omega_2^{\oplus}$ associated to section 3. Since $\omega_2^{\mathrm{F}} \le \omega_2^{\oplus} = \omega_2^{\alpha}$ (see Figure 2), from Appendix A.4, it can be concluded that $\omega_2^{\mathrm{F}} \le \omega_2^{\beta} \le \omega_2^{\oplus}$. Consider again eq 84 and observe that the first addendum in the right-hand side is zero, the second factor of the second addendum is again negative, whereas the left-hand side is negative because $\omega_2^{\beta} \le \omega_2^{\oplus}$, and $F(\omega)$ is monotonically increasing in the interval between H_1 and H_2. It follows that $(m_3\delta_3 - \omega_2^{\beta})$ is also negative. Since $m_3\delta_3 = \omega_1^{\oplus}$, it follows that $\omega_1^{\oplus} < \omega_2^{\beta} \le \omega_2^{\oplus}$ and the constraint under consideration is always fulfilled.

The complete separation region for the Langmuir isotherm is shown in Figure 5; it is delimited by three straight lines and one curve as indicated also in Table 5. It is worth noting that only the portion between points **r** and $\mathbf{w}_{\mathrm{L}}$ of the line **rw** belongs to the boundary of the complete separation region, whereas the segment **rf** lies within the region. It is also worth noting that along the whole line between **f** and $\mathbf{w}_{\mathrm{L}}$ ω_2^{F} is a root of eq 48; however, between $\mathbf{w}_{\mathrm{L}}$ and **r**, $\omega_2^{\mathrm{F}} = \omega_2^{\oplus} = \omega_2^{\gamma} > \omega_2^{\ominus}$. In point **r**, the two roots coincide and are equal to ω_2^{F}, whereas $\omega_2^{\mathrm{F}} = \omega_2^{\ominus} < \omega_2^{\gamma}$ along the segment **rf**. In the case of the Langmuir isotherm, the results reported here are not new, since they have been reported earlier; however, it is noteworthy that the method to derive them adopted here is different and more general.

4.2.3. Anti-Langmuir Isotherm, Case A. Also, in the case of the anti-Langmuir isotherm, there are seven constraints to be fulfilled, as reported in Table 2, four of which are shared with case $\mathbf{M}_1$. In particular, the constraint associated to section 3, i.e., $\omega_1^{\oplus} \le H_2$, leads to eq 81 and to the line **aw** in Table 3; $\omega_2^{\oplus} \le \omega_2^{\mathrm{F}}$ holds true if the previous inequality is fulfilled; $\omega_1^{\ominus}$ and $\omega_2^{\oplus}$ attain their lower bound values only along the line **ab**.

The remaining three constraints are somehow symmetric to those considered for the Langmuir isotherm and can be treated similarly. The left-hand inequality associated to section 3 imposes that eq 47 have real roots, i.e., that its discriminant be nonnegative as stated by eq 53. Arguing as in the case of eq

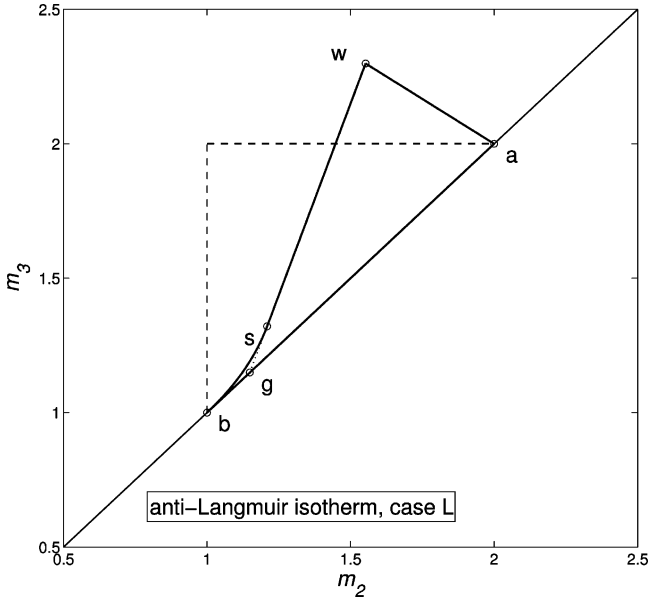

Figure 6. Region of complete separation in the (m_2, m_3) plane for the anti-Langmuir isotherm, case **A**. The parameters are as follows: $H_1 = 1$, $H_2 = 2$, $K_1 = 0.1$ L/g, $K_2 = 0.2$ L/g, $c_1^F = c_2^F = 2$ g/L. The dashed lines define the linear complete separation region.

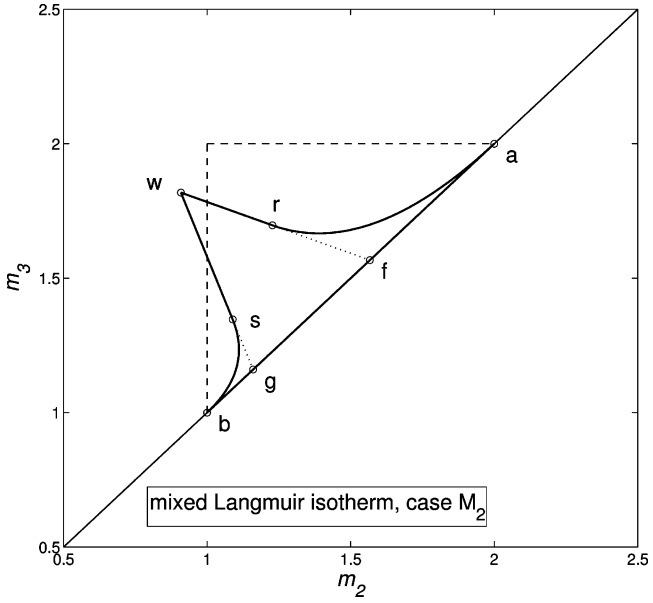

Figure 7. Region of complete separation in the (m_2, m_3) plane for the mixed Langmuir isotherm, case $\mathbf{M}_2$. The parameters are as follows: $H_1 = 1$, $H_2 = 2$, $K_1 = 0.1$ L/g, $K_2 = 0.2$ L/g, $c_1^F = c_2^F = 1$ g/L. The dashed lines define the linear complete separation region.

85, the last equation can be recast as

$$B_1 \geq 2\sqrt{C_1} \geq 0 \tag{87}$$

which is fulfilled in all points above the curve **bs** in Table 3. This represents a parabola in the (m_2, m_3) plane that belongs to the half plane $m_3 \geq m_2$ and is tangent to the diagonal $m_3 = m_2$ in the point **b** of Table 4.

The upper bound constraint on $\omega_1^{\ominus}$ yields an active constraint as well, which can be written as

$$f_1(\omega_1^F) = (\omega_1^F)^2 - B_1\omega_1^F + C_1 \leq 0 \tag{88}$$

This constraint is fulfilled by points on the right-hand side of the straight line **sw** given by the equation reported in Table 3, which is obtained by substituting eq 13 into the last equation. Such a straight line intersects the straight line **aw** in the optimal point $\mathbf{w}_A$ and the diagonal in point **g**; moreover, it is tangent to the curve **bs** in point **s**. Note that $\omega_1^F = \omega_1^{\ominus}$ along **sw** and $\omega_1^F = \omega_1^{\oplus}$ along the portion of that straight line between points **s** and **g**.

Finally, it is possible to demonstrate that the constraint $\omega_1^{\ominus} \leq \omega_2^{\ominus}$ associated to section 2 is always fulfilled since $\omega_1^{\ominus} = \omega_1^{\beta} \leq \omega_1^F$. This can be proved by using the results of Appendix A.4 and eq 83.

The complete separation region for the anti-Langmuir isotherm has a boundary made of four lines and is shown in Figure 6. It is worth noting that its features highlight a striking symmetry with the Langmuir case.

4.2.4. Mixed Langmuir Isotherm, Case $\mathbf{M}_2$. All the eight constraints reported in Table 2 for the mixed Langmuir isotherm $\mathbf{M}_2$ have already been discussed in one or the other of the previous cases. Those on $\omega_1^{\ominus}$ and $\omega_2^{\oplus}$ are the same as those for cases **A** and **L**, respectively. Similarly, those associated to sections 2 and 3 on $\omega_2^{\ominus}$ and $\omega_1^{\oplus}$, respectively, are a combination of those for cases **L** and **A**. Each of the eight constraints can be analyzed in the same way as in the cases above, thus reaching the same conclusions. In particular and with reference to Tables 3 and 5, the constraints on $\omega_1^{\ominus}$ lead to lines **ab** and **sw**; those on $\omega_2^{\oplus}$ lead to line **rw** and again to line **ab**; the left-hand side constraint on $\omega_2^{\ominus}$ is automatically fulfilled, whereas the right-hand side constraint is associated to line **ar**; the lower bound constraint on $\omega_1^{\oplus}$ leads to line **bs**, while, on the other hand, its upper bound constraint is always fulfilled.

The complete separation region for case $\mathbf{M}_2$ is shown in Figure 7; its boundary consists of five lines, and the optimal operating point, i.e., $\mathbf{w}_{M2}$ in Table 4, is at the intersection of lines **rw** and **sw**. Interestingly, along these two lines, $\omega_2^{\oplus} = \omega_2^F$ and $\omega_1^{\ominus} = \omega_1^F$, respectively. Both conditions hold in the optimal point $\mathbf{w}_{M2}$ and only there, thus implying that for optimal operating conditions the composition state of the γ stream (see Figure 2) is the same as that of the feed. Since under these circumstances also streams α and β have the same composition as the feed stream, it can be concluded that the feed state floods the whole portion of the TMB unit that connects sections 2 and 3. This can happen because for the mixed Langmuir isotherm $\mathbf{M}_2$ the transitions connecting the feed state to the steady states in both sections 2 and 3 are shock discontinuities.

5. Concluding Remarks

This paper contributes in at least two ways to the theory and practice of simulated moving bed chromatography. From a theoretical and conceptual point of view, exact criteria to achieve complete separation in binary SMB separations have been developed for the four different generalized Langmuir isotherms. Although the competitive Langmuir isotherm is one of the four and for it these criteria were already established, the need to extend them to a broader class of isotherms has imposed the use of new tools and methods, which bear a more general validity. The parallel derivation of the criteria for the four isotherms through the equilibrium theory is sounder and clearer and leads to a deeper understanding of the interrelation among the composition states within the TMB unit and of the interplay between complete separation requirements in the four sections of the unit.

From a practical point of view, the shape and position of the complete separation region in the operating parameter space can

be determined through simple algebraic relationships for all four generalized Langmuir isotherms. This allows understanding the SMB behavior in the case of systems subject to rather different retention behavior of the components to be separated. The qualitative and quantitative features of the complete separation region indicate major differences in the four cases and demonstrate that the existing criteria valid for the classical Langmuir isotherm would be misleading when used for a different isotherm. The results reported in this paper allow prediction of the effect of feed composition on the complete separation region in all four cases, hence providing important guidelines for SMB practitioners also in the cases where the parameters in the adsorption isotherm are not known very accurately. For the sake of brevity, the study of feed composition effects, which can be carried out using the relationships demonstrated here, has been reported elsewhere.[20] The analogies between the established design criteria for the competitive Langmuir isotherm and those reported here for the generalized Langmuir isotherm guarantee the possibility of extending to the new isotherm results obtained earlier for the Langmuir isotherm about robustness and optimization,[8] the effect of column efficiency,[21] the effect of extra-column dead-volume,[22] gradient SMB operations,[13−15]and SMB control.[4,5]

Appendix A

The objective of this appendix is to prove a number of useful inequalities on the ω_i values characterizing the composition states of different streams in a moving bed chromatographic column and in a TMB unit. The results are based on the properties of the function $F(\omega)$ in relation to different material balances that can be written for moving beds and TMBs.

The function $F(\omega)$ defined by eq 8 has two vertical asymptotes at H_1 and H_2; its value $F(0) = p_1n_1/N_1 + p_2n_2/N_2 = (p_1K_1c_1 + p_2K_2c_2)/\delta$ is smaller than 1 for all generalized Langmuir isotherms. $F(\omega)$ approaches zero for $\omega \rightarrow \pm\infty$; its derivative is always positive in case **L**, always negative in case **A**, positive for $\omega < H_1$ and negative for $\omega > H_2$ in case $\mathbf{M}_1$, and changes sign from negative to positive in case $\mathbf{M}_2$ (first region).[18] When comparing these properties with the ranges given by eqs 9−12, it can be noted that the function $F(\omega)$ is monotonic increasing or decreasing in all the intervals where it equals 1, i.e., where the characteristic parameters ω_1 and ω_2 are found, except in case $\mathbf{M}_2$ (first region), where $F(\omega)$ has a minimum in the interval of interest, i.e., between H_1 and H_2.

Since $p_1n_1/N_1 + p_2n_2/N_2 = 1 - 1/\delta$, then the following relationship holds:

$$\delta(F(\omega) - 1) = \omega\left(\frac{p_1K_1c_1}{H_1 - \omega} + \frac{p_2K_2c_2}{H_2 - \omega}\right) - 1 \qquad (89)$$

Using this, it is also possible to show that

$$\omega\left(1 + \frac{p_1K_1(mc_1 - n_1)}{H_1 - \omega} + \frac{p_2K_2(mc_2 - n_2)}{H_2 - \omega}\right) - m = (m\delta - \omega)(F(\omega) - 1) \qquad (90)$$

These equations are used in the following together with eqs 29 and 30 to prove a number of important properties of the ω values in a countercurrent column and in a TMB.

A.1. Let us first consider the case where the state *B* and the steady state (state *A* and the steady state) share the same ω^* value. Here, $F^B(\omega^*) = F^{ss}(\omega^*) = 1$ ($F^A(\omega^*) = F^{ss}(\omega^*) = 1$) and the rhs of eq 29 (the rhs of eq 30) is calculated where $\omega = \omega^*$ is zero. Therefore, also $F^b(\omega^*) = 1$ ($F^a(\omega^*) = 1$); hence, also state *b* (also state *a*) maps onto the same ω^*.

Let us now consider the case where the inlet and outlet states at one end of the column share the same ω^* value, i.e., $F^B(\omega^*) = F^b(\omega^*) = 1$ ($F^A(\omega^*) = F^a(\omega^*)$). Substituting these conditions in eq 29 (in eq 30) leads to the conclusion that either $F^{ss}(\omega^*) = 1$ or $m\delta_{ss} = \omega^*$, i.e., either the same ω^* value characterizes also the steady state or a very specific condition on the flow rate ratio must be fulfilled for such a situation to occur.

A.2. Here, it will be demonstrated that the ω values characterizing the outlet fluid and solid streams from a countercurrent adsorption column fulfill the following constraints:

$$\min\{\omega_i^B,\omega_i^{ss}\} \le \omega_i^b \le \max\{\omega_i^B,\omega_i^{ss}\} \quad (i = 1, 2) \qquad (91)$$

$$\min\{\omega_i^A,\omega_i^{ss}\} \le \omega_i^a \le \max\{\omega_i^A,\omega_i^{ss}\} \quad (i = 1, 2) \qquad (92)$$

A.2.1. Right End of the Column. We now proceed with the proof by considering first the right end of the column and the parameters ω_i^b. Note that the case where $\omega_i^{ss} = \omega_i^B$ for $i = 1$ or $i = 2$ fulfills the above equations thanks to the property proved in appendix A.1. Let us therefore assume that $\omega_i^B \neq \omega_i^{ss}$; this implies that $(F^B(\omega_i^{ss}) - 1)(F^{ss}(\omega_i^B) - 1) < 0$ (which of the two terms between brackets is positive depends on whether $F(\omega)$ is increasing or decreasing and on which between ω_i^B and ω_i^{ss} is larger).

With reference to eq 29, it can also be observed that the term $(m\delta_{ss} - \omega_i^B)$ is always nonnegative in the cases of interest here. This can be proven by considering inequalities 21−25 and noting that

(1) in the case where state B prevails at steady state, hence inequality 21 applies, then the simplified analysis of A.1 leads to the conclusion that $\omega_i^b = \omega_i^B$;

(2) where eq 22 holds, then $\omega_2^{ss} = \omega_2^B = \omega_2^b$ and $m\delta_{ss} = \omega_1^{T_1} > \omega_1^B$;

(3) in the case where the intermediate state prevails at steady state, then $\omega_2^{ss} = \omega_2^B = \omega_2^b$ and $m\delta_{ss} \ge \omega_1^B$, due to inequality 23;

(4) where eq 24 holds, then $m\delta_{ss} = \omega_2^{T_2} > \omega_2^B > \omega_1^B$;

(5) in the case where state A prevails at steady state, then $m\delta_{ss} \ge \omega_2^B > \omega_1^B$, due to inequality 25.

On the basis of these observations, eq 29 leads to the conclusion that for $i = 1$, 2 the groups $(F^b(\omega_i^{ss}) - 1)$ and $(F^b(\omega_i^B) - 1)$ have the same sign as the groups $(F^B(\omega_i^{ss}) - 1)$ and $(F^{ss}(\omega_i^B) - 1)$, respectively; hence, they have opposite sign. This finding implies that $F(\omega_i^b) = 1$ for a value ω_i^b, which fulfills eq 91, as it was to be demonstrated.

A.2.2. Left End of the Column. Let us consider the left end of the column, eq 30, and the parameters ω_i^a, and let us follow the same logic as for the right end of the column. Assuming $\omega_i^A \neq \omega_i^{ss}$ yields $(F^A(\omega_i^{ss}) - 1)(F^{ss}(\omega_i^A) - 1) < 0$, i.e., the two groups between brackets have opposite sign. Moreover, the term $(m\delta_{ss} - \omega_i^A)$ is always nonpositive in the cases of interest, as it can be shown by considering inequalities 21−25 and noting that

(1) in the case where state A prevails at steady state, hence inequality 25 applies, then the simplified analysis of A.1 leads to the conclusion that $\omega_i^a = \omega_i^A$;

(2) where eq 24 holds, then $\omega_1^{ss} = \omega_1^A = \omega_1^a$ and $m\delta_{ss} = \omega_2^{T_2} < \omega_2^A$;

(3) in the case where the intermediate state prevails at steady state, then $\omega_1^{ss} = \omega_1^A = \omega_1^a$ and $m\delta_{ss} \le \omega_2^A$, due to inequality 23;

(4) where eq 22 holds, then $m\delta_{ss} = \omega_1^{T_1} < \omega_1^A < \omega_2^A$;

(5) in the case where state B prevails at steady state, then $m\delta_{ss} \le \omega_1^A < \omega_2^A$, due to inequality 21.

When applied to eq 30, these observations allow drawing the conclusion that the groups $(F^a(\omega_i^{ss}) - 1)$ and $(F^A(\omega_i^A) - 1)$ $(i = 1, 2)$ have the same sign as the groups $(F^A(\omega_i^{ss}) - 1)$ and $(F^{ss}(\omega_i^A) - 1)$, respectively; hence, they have opposite sign. Therefore. $F(\omega_i^a) = 1$ for a value ω_i^a that fulfills inequality 91, as it was to be demonstrated.

A.3. In this section, we consider cases where one of the two species enters only from one end of a countercurrent column and derive conditions that guarantee that it does not leave the column from the other end.

A.3.1. Right End of the Column. We assume that the *B* stream at the right end of the column contains only species 1; hence, one of the ω_i^B values equals H_2, whereas both species are present in the *A* stream at the left end of the column. Note that the net flux of species 2 is proportional to $f_2 = (m\delta_{ss} - H_2)c_2^{ss}/\delta_{ss}$ according to eq 26. It is quite obvious that if species 2 is not present at steady state in the column, i.e., when according to inequalities 21−25 either state *B*, state T_1, or state *I* prevails at steady state and $\omega_i^{ss} = H_2$ for $i = 1$ or 2, then the rhs of eq 27 equals zero and $c_2^b = 0$, as required. In the following, we prove that $c_2^{ss} = 0$ is a necessary and sufficient condition to have $c_2^b = 0$.

Let us consider the case where the state characterizing the *B* stream is (ω_1^B, H_2) and $\omega_2^{ss} \neq H_2$. If state *A* prevails at steady state, then $(m\delta_{ss} - H_2) \ge \max\{\omega_2^A, H_2\} - H_2 \ge 0$ due to inequality 25. If state T_2 prevails, then $(m\delta_{ss} - H_2) = \omega_2^{T_2} - H_2 > 0$ due to eq 24. In the case where the *B* stream is characterized by (H_2, ω_2^B) (which is possible only for the isotherm **A**) and $\omega_1^{ss} = \omega_1^A$ (since $H_2 = \omega_1^B > \omega_1^A$, the first transition is a shock and state T_1 is not feasible), then $(m\delta_{ss} - H_2) \ge \max\{\omega_1^A, H_2\} - H_2 = 0$ due to eq 23. In all these three cases, $f_2 \ge 0$ and the rhs of eq 27 would be such that $c_2^b \ge 0$, which is not allowed. It is worth noting that the fact that $f_2 = c_2^b = 0$ is possible also where $m\delta$ takes its lower bound value does not disprove the property that $c_2^{ss} = 0$ is a necessary and sufficient condition for $c_2^b = 0$. In these limit cases in fact, the relevant transition is a shock and when $m\delta$ is at its lower bound the shock is standing, i.e., its propagation velocity is zero, and the two states on the two sides of the shock, one of which being that where $c_2^{ss} = 0$, coexist at steady state.

A.3.2. Left End of the Column. Let us consider the symmetric situation where the *A* stream at the left end of the column contains only species 2 and $\omega_i^A = H_1$ for $i = 1$ or 2. On the contrary, both species are present in the *B* stream; the net flux of species 1, f_1, is proportional to $(m\delta_{ss} - H_1)$ according to eq 26. If species 1 is not present at steady state in the column, i.e., when according to inequalities 21−25 either state *A*, state T_2, or state *I* prevails at steady state and $\omega_i^{ss} = H_1$ for $i = 1$ or 2, then the rhs of eq 28 equals 0 and $c_1^a = 0$, as required. Below, it is demonstrated that $c_1^{ss} = 0$ is a necessary and sufficient condition for $c_1^a = 0$.

In the case where the state characterizing the *A* stream is (H_1, ω_2^A) and $\omega_1^{ss} \neq H_1$, the following two subcases have to be considered: if state *B* prevails at steady state, then $(m\delta_{ss} - H_1) \le \min\{\omega_1^B, H_1\} - H_1 \le 0$ due to inequality 21; if state T_1 prevails, then $(m\delta_{ss} - H_1) = \omega_1^{T_1} - H_1 < 0$ due to eq 22. Let us consider the case where the *A* stream is characterized by (ω_1^A, H_1) (which is possible only for the isotherm **L**) and $\omega_2^{ss} = \omega_2^B$ (since $H_1 = \omega_2^A < \omega_2^B$, the second transition is a shock and state T_2 is not feasible), then $(m\delta_{ss} - H_1) \le \min\{\omega_2^B, H_1\} - H_1 = 0$ due to eq 23. In all the cases above, $f_1 \le 0$ and the rhs of eq 28 would be such that $c_1^a \le 0$, contrary to what is required. Likewise, the case considered in the previous section about the right end of the column and based on the same argument, also in this case the possibility of having $f_1 = c_1^a = 0$ when $m\delta$ attains its upper bound is consistent with $c_1^{ss} = 0$ being a necessary and sufficient condition for $c_1^a = 0$.

A.3.3. Other Cases. Also in the single component case where one solute enters at one end of the column, whereas pure solvent is fed from the other, similar conclusions can be reached, namely, that pure solvent must prevail in the column at steady state to avoid the solute reaching the opposite column end.

A.4. In the following, we consider the mixing process of two streams at a node of a separation unit, e.g., the feed node in the unit of Figure 2, and we prove that the ω_i values characterizing the resulting stream are bracketed by the corresponding ones of the incoming streams.

The single component material balances at a mixing node, where the fluid streams I and II mix yielding stream *M*, can be written as follows:

$$c_i^M = \alpha c_i^{I} + (1 - \alpha)c_i^{II} \quad (i = 1, 2) \tag{93}$$

where $0 \le \alpha \le 1$. Multiplying eq 93 by $p_iK_i/(H_i - \omega)$, summing them, and then multiplying by ω on both sides of the resulting expression yields the following equation, whose solutions give the values of ω associated to the mixed state *M*, i.e., ω_i^M:

$$\delta_M(F^M(\omega) - 1) = \alpha\delta_I(F^I(\omega) - 1) + (1 - \alpha)\delta_{II}(F^{II}(\omega) - 1) \tag{94}$$

By reasoning as in appendix A.2, it can be readily concluded that

$$\min\{\omega_i^I, \omega_i^{II}\} \le \omega_i^M \le \max\{\omega_i^I, \omega_i^{II}\} \quad (i = 1, 2) \tag{95}$$

A.5. Let us now consider the four-section unit shown in Figure 2. We can see that, with only the exception of the two incoming streams (i.e., feed and desorbent), each stream in the unit may be regarded as derived from the others in one of the two following ways. The constant state inside each column as well as all the outgoing streams can be determined from the composition of the incoming streams, using the solution of the single section problem outlined above. Similarly, the streams leaving the mixing nodes (at the feed and desorbent inlets) are determined by the two inlet streams. In both cases, the results demonstrated in this appendix A show that the obtained ω_i values are bounded by those of the incoming streams. Since this applies to all streams in the unit except the feed and desorbent, by recursively using this result, we can derive condition 32.

Appendix B

This appendix aims at establishing that some types of states cannot be attained at steady state in a TMB unit, since they would lead to a violation of the process specifications.

B.1. The inequalities reported in Table 1 are a special case of the general inequalities of eqs 21−25; they enforce the constraints that make it possible to achieve the steady states illustrated in the TMB schematic of Figure 2. Filling in Table 1 requires that one establish in a unique manner for every section of the TMB unit which of the ω_i values of the two incoming states, i.e., the fluid from the left and the solid from the right (see Figure 3), is larger. On the basis of eqs 9−12, this

assessment is straightforward when one of the ω values is either H_1 or H_2, i.e., in sections 1 and 4.

In the other cases, one can proceed as follows. Let us consider section 2 first, and the question whether ω_2^E is larger than ω_2^γ or not. In cases **L** and $\mathbf{M}_2$, eq 91 applied to the right end of section 1 together with eqs 9 and 12 yields $\omega_2^{ES} \leq \omega_2^E \leq H_2$. Equation 92 applied to the left end of section 2 is consistent with the last inequalities, if and only if $\omega_2^E > \omega_2^\gamma$. In cases **A** and $\mathbf{M}_1$ on the contrary, one concludes from a balance at the right end of section 1 that $H_2 \leq \omega_2^E \leq \omega_2^{ES}$, due to eqs 10 and 11, and then from eq 92 applied to the left end of section 2 that $\omega_2^E < \omega_2^\gamma$.

Repeating the same analysis for section 3, one concludes that $\omega_1^{RS} > \omega_1^\gamma$ in cases **L** and $\mathbf{M}_1$, whereas $\omega_1^{RS} < \omega_1^\gamma$ in cases **A** and $\mathbf{M}_2$.

B.2. Here, it is demonstrated that the extract state cannot prevail at steady state in either section 1 or section 2; likewise, the raffinate state cannot prevail in either section 3 or section 4.

Let us consider the extract node first, where under complete separation conditions component 1 is absent, and observe that, based on the analysis in appendix A.1, if the extract state prevails in either section 1 or section 2, then the ω_2 values of the states in section 1, in section 2, at the extract outlet, and at the solid outlet of section 2 must be the same, i.e., $\omega_2^1 = \omega_2^E = \omega_2^{ES} = \omega_2^2$. Moreover, complying with conditions 23 and 25 implies that $m_1\delta_1 \leq \min\{\omega_2^E, H_2\}$ and $m_2\delta_2 \geq \max\{\omega_2^E, \omega_2^\gamma\}$, respectively. Applying the results of appendix B.1 leads on one hand to the conclusion that in cases **L** and $\mathbf{M}_2$ the net flux of component 2 in section 1 is negative, since $f_2^1 \propto (m_1\delta_1 - H_2) \leq (H_2 - H_2) = 0$; this would cause leakage of component 2 from section 1 into section 4, thus polluting the raffinate. On the other hand, in cases **A** and $\mathbf{M}_1$, the net flux of species 2 in section 2 is positive, which is unacceptable since it would not allow the collection of any species 2 in the extract, which would be flooded with solvent phase; this happens because $f_2^2 \propto (m_2\delta_2 - H_2) \geq (\omega_2^\gamma - H_2) > 0$.

Let us apply a similar line of reasoning to the raffinate node. If the raffinate state prevails in either section 3 or section 4, then $\omega_1^4 = \omega_1^R = \omega_1^{RS} = \omega_1^3$. It is straightforward to show that in this case the complete separation conditions would be violated in section 3 in the case of isotherms **L** and $\mathbf{M}_1$ and in section 4 in the cases **A** and $\mathbf{M}_2$.

B.3. The aim of this section is to show that certain transition states can indeed prevail at steady state in sections 2 and 3 but that the corresponding operating points, i.e., the corresponding values of the flow rate ratios m_2 and m_3, belong to the boundary of the complete separation regions calculated, assuming that the states prevailing at steady state are those in Figure 2, where the transition states are not considered.

Such situation may occur in section 2 if the transition state between the extract state characterized by the ω values (H_1, ω_2^E) and the intermediate state (H_1, ω_2^γ) prevails at steady state. This is possible for isotherms **L** and $\mathbf{M}_2$, if according to eq 24 $m_2\delta_2 = \omega_2^{T_2}$ with $\omega_2^E < \omega_2^{T_2} < \omega_2^\gamma = \omega_2^\oplus$. Since in this case $\delta_2 = H_2/\omega_2^{T_2}$, this condition implies $m_2H_2 = (\omega_2^{T_2})^2$. Considering these relationships in the light of eqs 48 and 52 leads to the conclusion that they are equivalent to $\omega_2^\ominus = \omega_2^\oplus$, which is the condition fulfilled along the line **ar** on the boundary of the complete separation regions for the isotherms **L** and $\mathbf{M}_2$. Therefore, all operating points associated to the transition state prevailing at steady state in section 2 belong to the line **ar**. The question is whether these points are only those between points **a** and **r** or are there more. With reference to Tables 3 and 4, note that between **a** and **r** the quantity $m_2H_2 = (\omega_2^{T_2})^2$ varies between $(\omega_2^F)^2$ and H_2^2, which means that $\omega_2^{T_2}$ varies within its whole feasible range of variability defined by relation 32. This completes the proof.

A similar argument can be repeated for the transitions state that might prevail in section 3 in the case of isotherms **A** and $\mathbf{M}_2$. It can be easily proved that all the corresponding operating points belong to the curve **bs** defined in Table 3.

Notation

a = outlet solid state from a moving bed adsorber
a = point on the boundary of the complete separation region, see Table 4
A = inlet fluid state to a moving bed adsorber
A = anti-Langmuir isotherm
b = outlet fluid state from a moving bed adsorber
b = point on the boundary of the complete separation region, see Table 4
B = inlet solid state to a moving bed adsorber
B_1, B_2 = coefficients defined by eqs 49 and 51
C_1, C_2 = coefficients defined by eqs 50 and 52
c_i = fluid phase concentration of component i
f_1, f_2 = functions defined by eqs 47 and 48
f_i^j = rescaled net flow rate of component i in section j, defined by eq 26
f = point on the boundary of the complete separation region, see Table 4
$F(\omega)$ = function defined by eq 8
F_i^j = net flow rate of component i in section j, defined by eq 26
g = point on the boundary of the complete separation region, see Table 4
h = parameter, defined as N_1/N_2
H_i = Henry's constant of component i, $H_i = K_iN_i$
I = intermediate state
k = parameter, defined as $(1 - H_1/H_2)/K_1$
K_i = adsorption equilibrium constant of component i
L = Langmuir isotherm
m = flow rate ratio, defined by eq 3
$\mathbf{M}_1$ = mixed Langmuir isotherm with $p_1 = 1 = -p_2$
$\mathbf{M}_2$ = mixed Langmuir isotherm with $p_1 = -1 = -p_2$
n_i = adsorbed phase concentration of component i
N_i = adsorbed phase saturation concentration of component i
p_i = parameter in the generalized Langmuir isotherm, $p_i = \pm 1$
Q_j = fluid volumetric flowrate in section j
Q_s = solid-phase volumetric flowrate in a TMB unit
r = point on the boundary of the complete separation region, see Table 4
s = point on the boundary of the complete separation region, see Table 4
t^* = switch time in a SMB unit
T = transition state
V = volume of the adsorption column
w = point on the boundary of the complete separation region, see Table 4
x = dimensionless axial coordinate

Greek Letters

α = coefficient used in eqs 93 and 94
δ = denominator in the generalized Langmuir isotherm, defined by eq 6
ϵ_b = interparticle void fraction
ϵ_p = intraparticle void fraction
ϵ^* = overall void fraction, $\epsilon^* = \epsilon_b + \epsilon_p(1 - \epsilon_b)$

η = parameter, defined as $\eta = \epsilon_p/(1 - \epsilon_p)$
τ = dimensionless time
ω = characteristic parameter defined as a root of eq 8

Subscripts and Superscripts

0 = initial state
cr = critical threshold
E = extract stream
ES = solid stream facing the extract port in the TMB unit
F = feed stream
i = component index
j = section index
R = raffinate stream
RS = solid stream facing the raffinate port in the TMB unit
SMB = SMB unit
ss = steady state in a moving bed adsorber
TMB = TMB unit
α = internal stream in the TMB unit
β = internal stream in the TMB unit
γ = internal stream in the TMB unit
$\ominus,\oplus$ = smaller and larger root, respectively, of quadratic eqs 47 and 48

Literature Cited

(1) Nicoud, R.-M. The separation of optical isomers by simulated moving bed chromatography (Part II). *Pharm. Technol. Eur.* **1999**, *11*, 28.

(2) Juza, M.; Mazzotti, M.; Morbidelli, M. Simulated moving-bed chromatography and its application to chirotechnology. *Tibtech* **2000**, *18*, 108.

(3) Schulte, M.; Strube, J. Preparative enantioseparations by simulated moving bed chromatography. *J. Chromatogr., A* **2001**, *906*, 399.

(4) Erdem, G.; Abel, S.; Morari, M.; Mazzotti, M.; Morbidelli, M.; Lee, J. Automatic Control of Simulated Moving Beds. *Ind. Eng. Chem. Res.* **2004**, *43*, 405.

(5) Abel, S.; Erdem, G.; Amanullah, M.; Morari, M.; Mazzotti, M.; Morbidelli, M. Optimizing control of Simulated Moving Beds-Experimental implementation. *J. Chromatogr., A* **2005**, *1092*, 2.

(6) Rhee, H.-K.; Aris, R.; Amundson, N. R. *First order partial differential equations*; Prentice-Hall: Englewood Cliffs, NJ, 1989; Vol. II.

(7) Storti, G.; Mazzotti, M.; Morbidelli, M.; Carrá, S. Robust design of binary countercurrent separation processes. *AIChE J.* **1993**, *39*, 471.

(8) Mazzotti, M.; Storti, G.; Morbidelli, M. Optimal operation of Simulated Moving Bed units for nonlinear chromatographic separations. *J. Chromatogr., A* **1997**, *769*, 3.

(9) Gentilini, A.; Migliorini, C.; Mazzotti, M.; Morbidelli, M. Optimal operation of Simulated Moving Bed units for nonlinear chromatographic separations. II Bi-Langmuir isotherms. *J. Chromatogr., A* **1998**, *805*, 37.

(10) Migliorini, C.; Mazzotti, M.; Morbidelli, M. Robust design of binary countercurrent separation processes 5. Non constant selectivity binary systems. *AIChE J.* **2000**, *46*, 1384.

(11) Chiang, A. S. T. Complete separation conditions for a local equilibrium TCC adsorption unit. *AIChE J.* **1998**, *44*, 332.

(12) Migliorini, C.; Mazzotti, M.; Morbidelli, M. Design of simulated moving bed multicomponent separations: Langmuir systems. *Sep.Purif. Technol.* **2000**, *20*, 79.

(13) Mazzotti, M.; Storti, G.; Morbidelli, M. Supercritical fluid simulated moving bed chromatography. *J. Chromatogr., A* **1997**, *786*, 309.

(14) Migliorini, C.; Wendlinger, M.; Mazzotti, M.; Morbidelli, M. Temperature gradient operation of a simulated moving bed unit. *Ind. Eng. Chem. Res.* **2001**, *40*, 2606.

(15) Abel, S.; Mazzotti, M.; Morbidelli, M. Solvent gradient operation of simulated moving beds: 2 Langmuir isotherms. *J. Chromatogr., A* **2004**, *1026*, 47.

(16) Paredes, G.; Abel, S.; Mazzotti, M.; Morbidelli, M.; Stadler, J. Analysis of a simulated moving bed operation for three-fraction separations (3F-SMB). *Ind. Eng. Chem. Res.* **2004**, *43*, 6157.

(17) Mihlbachler, K.; Seidel-Morgenstern, A.; Guiochon, G. Detailed study of Tröger's base separation by SMB process. *AIChE J.* **2004**, *50*, 611.

(18) Mazzotti, M. Local equilibrium theory for the binary chromatography of species subject to a generalized Langmuir isotherm. *Ind. Eng. Chem. Res.* **2006**, *45*, 5232.

(19) Mazzotti, M. Delta-shock, a new type of composition front in nonlinear chromatography. *Ind. Eng. Chem. Res.* **2006**, in preparation.

(20) Mazzotti, M. Equilibrium theory based design of Simulated Moving Bed processes for a generalized Langmuir isotherm. *J. Chromatogr., A* **2006**, in press.

(21) Migliorini, C.; Gentilini, A.; Mazzotti, M.; Morbidelli, M. Design of simulated moving bed units under nonideal conditions. *Ind. Eng. Chem. Res.* **1999**, *38*, 2400.

(22) Migliorini, C.; Mazzotti, M.; Morbidelli, M. Simulated moving bed units with extracolumn dead volume. *AIChE J.* **1999**, *45*, 1411.

Received for review March 11, 2006
Revised manuscript received June 3, 2006
Accepted June 27, 2006

IE060298N